Gas generation mechanism due to electrolyte decomposition in commercial lithium-ion cell

Kazuma Kumai *, Hajime Miyashiro, Yo Kobayashi, Katsuhito Takei, Rikio Ishikawa

Central Research Institute of Electric Power Industry (CRIEPI), 2-11-1, Iwado Kita, Komae-shi, Tokyo 201-8511, Japan

Abstract

To elucidate the gas generation mechanism due to electrolyte decomposition in commercial lithium-ion cells after long cycling, we developed a device which can accurately determine the volume of generated gas in the cell. Experiments on $Li_xC_6/Li_{1-x}CoO_2$ cells using electrolytes such as 1 M $LiPF_6$ in propylene carbonate (PC), dimethyl carbonate (DMC), ethyl methyl carbonate (EMC), and diethyl carbonate (DEC) are presented and discussed. In the nominal voltage range (4.2–2.5 V), compositional change due mainly to ester exchange reaction occurs, and gaseous products in the cell are little. Generated gas volume and compositional change in the electrolyte are detected largely in overcharged cells, and we discussed that gas generation due to electrolyte decomposition involves different decomposition reactions in overcharged and overdischarged cells. © 1999 Elsevier Science S.A. All rights reserved.

Keywords: Commercial lithium-ion cell; Gas generation mechanism; Electrolyte decomposition; Long cycling

1. Introduction

The demand for long-life energy storage battery systems has been increasing [1]. One sample of such cells is a lithium-ion cell in which carbon materials and Li_xCoO_2 are used as negative and positive active materials, respectively. The electrolytes generally used in these cells are cyclic alkyl carbonate and chain alkyl carbonate solution, with $LiPF_6$ as a salt. It was reported that gas generation due to electrolyte decomposition occurs in these cells during cycling [2–4]. Electrolyte stability, in particular, is important for long life and safety of cells in practical use [5]. Therefore, one of the important issues in the development of a long-life and safe lithium-ion cell is the estimation of the decomposition and compositional change of electrolytes during long cycling. However, the degradation mechanism remains to be understood in commercial cells.

In this study, we carried out long-life cycle tests, and electrolyte decomposition was investigated by means of analysis of the generated gases in the cell, in order to investigate the degradation mechanism of the 1 Ah capacity commercial lithium-ion cell.

2. Experimental

2.1. Test cells

One ampere hour capacity commercial lithium-ion cells (US18650 from an NP-500 battery pack), commercialized by Sony for video equipment, were used as samples. These cells have a carbon anode, a $LiCoO_2$ cathode, and an electrolyte solution containing 1 M $LiPF_6$ dissolved in a mixture of propylene carbonate (PC), ethyl methyl carbonate (EMC), diethyl carbonate (DEC) and dimethyl carbonate (DMC).

In this study, the cells were cycled as follows: (1) long cycling in the nominal voltage range (4.2–2.5 V) at various charge and discharge rates, and (2) imbalanced cells pre-shifted by +5% and −10% of the capacities compared to the standard cell were used for overcharge and overdischarge tests. The cells were operated for a number of cycles at constant capacity without voltage limitation. All test cells were maintained at 25°C during the cycles.

2.2. Determination of generated gas volume

To determine the volume of generated gas in the cell, an apparatus was constructed as shown in Fig. 1. It was composed of: (1) a vessel to release and hold of generated

* Corresponding author. Tel.: +81-3-3480-2111; Fax: +81-3-3488-6697; E-mail: kuami@criepi.denken.or.jp
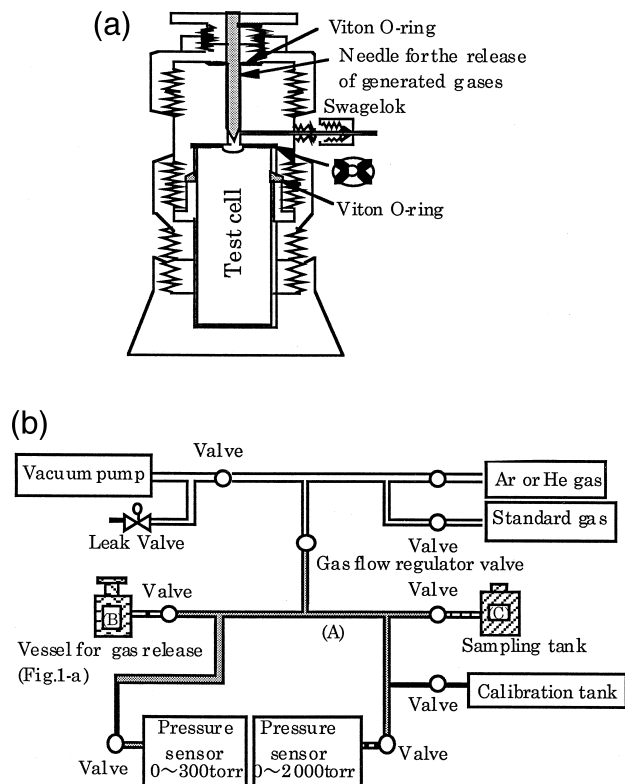
Fig. 1. (a) Schematic drawing of a vessel for the release of generated gases in the cells. (b) Schematic diagram of the apparatus for gas volume measurements.

gas in the cell (Fig. 1a), (2) a pressure sensor to measure released and dilution gas volume, (3) a sampling tank to buffer pressure fluctuation and analyze, and (4) a vacuum pump to evacuate before and after measurement. The apparatus is a closed and sealed system. After cycle tests, the cells were placed in the vessel after drilling a hole 4 mm in diameter at the center of the positive terminal cap, and vacuumed until approximately 0.1 Torr. The gases generated in the cells were then released into the vessel

puncturing by the needle. Using this device, the volume of generated gas in the cell can be measured directly. The total volume of gas was calculated from the pressure and the space volume in each part of the apparatus. This method can determine up to 0.01 ml in volume.

2.3. Analysis of gas and electrolyte composition

The composition of the sampled gas was analyzed by gas chromatography (Shimadzu GC-14A). A flame ionization detector (FID) was used to detect hydrocarbons, and a thermal conductive detector (TCD) was also used to detect inorganic gas in the generated gases. As sample, 0.5 ml of gas was injected for the abovementioned analyses.

The cells were then removed from the gas release vessel, and added organic solvent (dichloromethane, 1 ml) for 30 min to leach electrolytes. The compositional change of the electrolytes was determined by gas chromatography/mass spectrometry (GC/MS; Hewlett-Packard, HP-5971A).

3. Results and discussion

3.1. Gas generation in the nominal voltage range

The cells were operated about 2500 cycles at different charge and discharge currents in the nominal voltage range, and changes in electrolyte composition and generated gas volume were examined. The composition of electrolyte before cycling was determined as PC (50%), EMC (25%), DEC (15%), and DMC (10%) in vol%. The compositional change of electrolyte was analyzed from comparison of each peak area with that of before cycled cell.

Table 1 shows the volume and the composition of generated gases after long cycling in the nominal voltage range. When the cells were operated for 2000–3000 cy-

Table 1
Composition of gases generated in the nominal operating voltage range (4.2 V–2.5 V), and during overcharging and overdischarging

Test no.	Test conditions		Cycle number	Capacity at end cycle (Ah)	Composition of detected gases (%)								Total volume (ml)
	Charge current	Discharge current			O_2	N_2	CO_2	CO	CH_4	C_2H_6	C_3H_8	C_3H_6	
R1	Before cycle test				5.3	42.5	1.7		40	4.2	0.4		0.95
R2		100 mA	2043	0.6	2.7	8.5	2.2		72	6.7	7.2	0.4	2.23
R3	200 mA	125 mA	2397	0.6	1.7	5.9	4.1		73	7.0	7.9	0.4	2.42
R4		200 mA	2331	0.5	1.5	6.5	7.2		61	7.6	15.6	0.8	2.63
R5		500 mA	2301	0.5	2.3	11.0	4.0		62	9.2	10.4	0.6	1.73
R6	125 mA		1915	0.6	2.1	7.7	1.3		75	7.8	6.2	0.2	2.01
R7	200 mA	125 mA	2570	0.5	3.2	6.6	3.2		72	8.3	7.2	0.4	2.78
R8	500 mA		3111	0.6	6.1	25.4	2.5		51	6.2	8.5	0.4	1.75
R9	200/200 mA, overcharge		880	0.6	1.3	5.3	75.6		12	2.6	2.7		10.57
R10	200/200 mA, overdischarge		880	0.0	0.3	1.5	71.2	0.6	21	3.2	0.8	1.0	40.21

cles, their capacity reduced by half. The total gas volume in the cycled cells was in the range of 1.7–2.8 ml, and mainly methane gas was detected. Trace amounts of ethane, propane, and other hydrocarbons were also detected. This shows that the decomposition of the electrolytes occurred in the cell during long cycling.

In nominal voltage range, the gas generation is considered to result from side reaction of ester exchange as follows.

$$ROCO_2R + Li^+ + e^- \rightarrow ROCO_2Li \downarrow + R^* \qquad (1)$$

$$ROCO_2Li + Li^+ + e^- \rightarrow Li_2CO_3 \downarrow + R^* \qquad (2)$$

$$R^* + 1/2H_2 \rightarrow Alkyl \uparrow \qquad (3)$$

$$R^* + R^* \rightarrow R\text{–}R \uparrow \qquad (4)$$

In the electrolyte solution, the concentration of PC was not changed, but that of EMC was reduced and those of both DEC and DMC were increased following cycles. This suggests that the change in composition of the electrolyte due to ester exchange reaction such as EMC → DMC + DEC occurs independent of the charge/discharge current. The ester exchange reaction in cells containing PC, DMC and DEC electrolytes was reported according to the following equation [6].

$$DEC + DMC \rightleftarrows 2EMC \qquad (5)$$

Our results indicate that the equilibrium was not established, and compositional change of electrolytes occurred following cycles. This reaction may affect the cell reaction which is related to the charged states of the cathode ($Li_{1-x}CoO_2$) and the anode (Li_xC_6). However, with the presence of both high-potential (cathode) and low-potential (anode) materials in a cell, it is difficult to distinguish which electrode is responsible for the ester exchange reaction in commercial lithium-ion cells.

3.2. Gas generation behavior

In the 5% overcharged state, the cell had about 4.3 V at the end of charge from the first cycle to the end of cycles. The 10% overdischarged cell reached 0 V at only about 50 cycles, it was short-circuit without venting. As shown in Table 1 (R9, R10), large volumes of carbon dioxide (CO_2), methane and other hydrocarbons were detected in the cells.
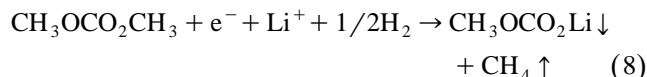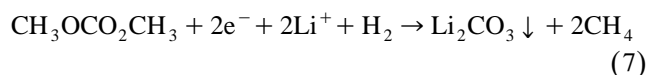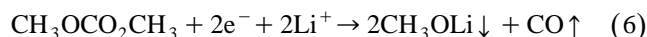
3.2.1. Gas generation in overdischarged cell

Large amount of CO_2 and hydrocarbons as well as CO were detected from overdischarged cell. No hydrogen was detected, but its detection was reported in similar electrolyte systems [3].

In the overdischarged state, the copper of the anode current collector dissolves at low potential range, and the cathode is plated with dissolved copper. Thus, no charging reaction occurred at the cathode, and electrolyte decomposition is accelerated. As a result, a large volume of hydrocarbon was produced. From these results, it was assumed that the decomposition of the electrolytes was mainly due

to the reduction of the electrolytes. This reaction seemed to be dependent on the change in surface conditions at the cathode.

For the case of DMC, gas generation reactions in the overcharged state cell are considered as follows.

$$CH_3OCO_2CH_3 + 2e^- + 2Li^+ \rightarrow 2CH_3OLi \downarrow + CO \uparrow \qquad (6)$$

$$CH_3OCO_2CH_3 + 2e^- + 2Li^+ + H_2 \rightarrow Li_2CO_3 \downarrow + 2CH_4 \qquad (7)$$

$$CH_3OCO_2CH_3 + e^- + Li^+ + 1/2H_2 \rightarrow CH_3OCO_2Li \downarrow + CH_4 \uparrow \qquad (8)$$

The case of DEC and EMC could be explained by similar reactions. These suggest that during overdischarging, the decomposition of electrolytes takes place with the release of hydrocarbons, CO, CO_2, and other gases.

3.2.2. Gas generation in overcharged cell

In a study on used cells, CO_2 generation at 4.8 V or above from lithium carbonate added in cathode was reported for the cells [7]. In our experiment, the cell did not reach that voltage. However, a large amount of CO_2 was detected in our overcharged cell. It was assumed that CO_2 was mainly generated due to the generation of oxygen (O_2) from cathode material during overcharging. As shown in Table 1 (R9), O_2 concentration was about 3 times that in other cells. This implies that O_2 was generated as a result of decomposition of the overcharged cathode material.

The mechanism of the generation of O_2 and CO_2 is considered as follows.

$$3CoO_2 \rightarrow Co_3O_4 + O_2 \uparrow \qquad (9)$$

$$CH_3OCO_2CH_3 (DMC) + 3O_2 \rightarrow 3CO_2 \uparrow + 3H_2O \qquad (10)$$
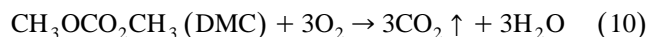
The reactions in (9) and (10) show O_2 generation due to the degradation of the cathode material and the decomposition of electrolytes by the generated O_2, respectively.
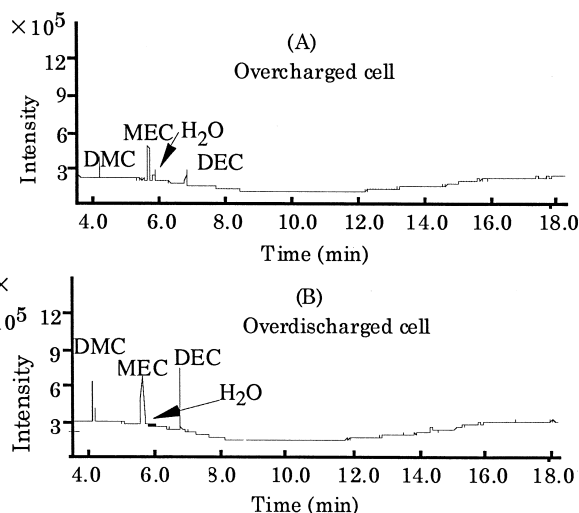

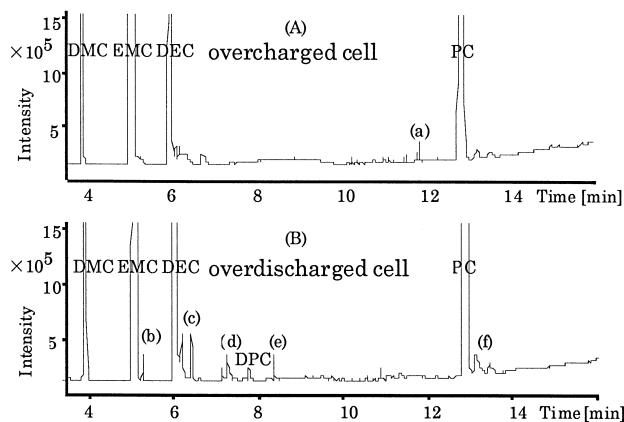Fig. 2. GC/MS chromatograms of the vapor in (A) overcharged cell and (B) overdischarged cell.

Fig. 3. GC/MS chromatograms of the electrolytes in (A) overcharged cell and (B) overdischarged cell. (a) Trimethyl and triethyl phosphate esters, (b) intermediate of EMC, (c) intermediate of DEC, (d) and (e) unknown, DPC: dipropyl carbonate, (f) intermediate of PC.

From GC/MS analysis of the vapor and electrolyte solutions in the overcharged cell, water (H_2O) and phosphate esters were detected as shown in Figs. 2 and 3, respectively. It is important that H_2O could be generated in the cell. H_2O leads many reactions in the cells.

Generation of R–O–R could be explained by hydrolysis of the esters producing alcohol and dehydration of the alcohol, if H_2O exists. From the electrolyte solution analysis, trimethyl and triethyl phosphate esters were detected. It was therefore suggested that $LiPF_6$ salt also degrades with overcharging.

3.3. Test conditions and generated gas volume

Fig. 4 shows the relationship between the generated volume of hydrocarbons and CO_2 in the cells. In the nominal voltage range, the volume of the gas generated was small, and the gases were almost exclusively hydrocarbons. Eliminating the short-circuit cell, the figure shows two different gas generation mechanisms due to electrolyte
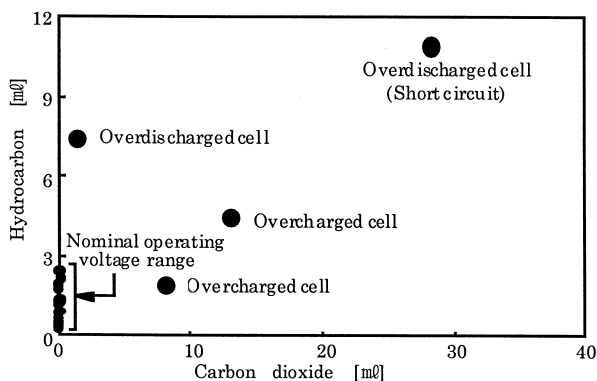

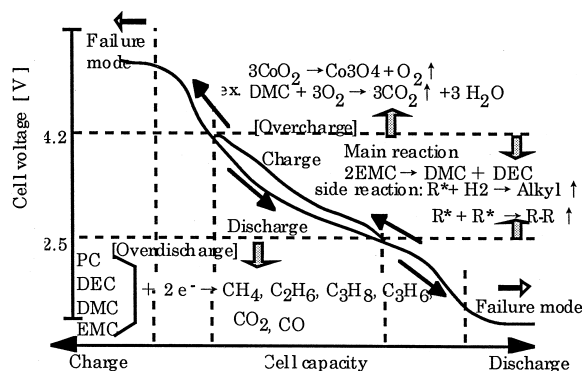Fig. 4. Relationship between generated hydrocarbons and carbon dioxide in the cell.

Fig. 5. Overcharge and overdischarge voltage profiles of Li-ion cell and the gas generation model.

decomposition in both overcharged and overdischarged cells. The results suggest that the decomposition of electrolytes in the overdischarged cell involved reduction, and generating mainly hydrocarbons. In the case of the overcharged cell, electrolyte decomposition involved oxidation due to oxygen generated from the cathode material, and generating CO_2 and hydrocarbons.

These events not only increase the internal pressure that can lead to safety hazards in practical cells, but also increase cell impedance, resulting in poor cell performance.

4. Conclusion

To investigate the mechanism of gas generation due to electrolyte decomposition, we developed a device which can accurately determine the volume of generated gases in the cell. From the analysis of the gases and electrolyte, the mechanism of gas generation due to electrolyte decomposition was discussed.

Fig. 5 shows the gas generation mechanism based on our results. In the nominal operating voltage range, compositional change mainly due to ester exchange occurs, but gaseous products in the cell are little. Large volumes of gas generation and large compositional change in the electrolyte are detected in overcharged and overdischarged cells, and we clarified that gas generation due to electrolyte decomposition involves different decomposition reactions in overcharged and overdischarged cells.

Acknowledgements

References

[1] Y. Tunoda, Sunshine J. 13 (2) (1993) .

[2] Z.X. Shu, R.S. McMillan, J.J. Murray, J. Electrochem. Soc. 140 (1993) 922.

[3] H. Yoshida, T. Fukunaga, T. Hazama, M. Terasaki, M. Mizutani, M. Yamachi, J. Power Sources 68 (1997) 311.

[4] E. Cattaneo, J. Ruch, J. Power Sources 43–44 (1993) 341.

[5] K.M. Abraham, D.H. Pasquariello, F.J. Maltin, J. Electrochem. Soc. 133 (1986) 661.

[6] E.S. Takeuchi, H. Gan, M. Palazzo, R.A. Leising, S.M. Davis, J. Electrochem. Soc. 144 (1997) 1944.

[7] K. Yamamoto, S. Nagaura, N. Kato, M. Nishi, 17th Advanced Battery Symposium in Japan, 170, 1992.